The 9th European Congress on Computational Methods in Applied Sciences and Engineering
ECCOMAS Congress 2024
3 – 7 June 2024, Lisboa, Portugal

A NUMERICAL STUDY OF FLUID-STRUCTURE INTERACTION FOR A FLEXIBLE FLAP IN TURBULENT FLOW

TAYYABA BANO[1], MARTIN HEINRICH[1] AND RÜDIGER SCHWARZE[1]

[1] Institute of Mechanics und Fluid Dynamics (imfd),
TU Bergakademie Freiberg,
Lampadiusstraße 4, D-09599 Freiberg, Germany,
e-mail: Tayyaba.bano@extern.tu-freiberg.de, www.tu-freiberg.de/fakult4/imfd

Key words: Flexible flap, fluid-structure interaction, deformation, bending, drag

Summary. *Our research work presents a numerical approach to examine the fluid-structure interaction (FSI) on a single flexible flap engrossed in an open water channel. The proposed method is specifically applied to investigate flow conditions of Reynolds number,* $700 < Re < 7000$. *The two-way coupled FSI method is employed to simulate the flap and flow behaviors and are compared with existing Particle Image Velocimetry (PIV) measurements. Three-dimensional (3D) transient simulations are performed using the commercial ANSYS Workbench. Both numerical and experimental data signify the mutual interaction of flexible flap and fluid. The flap experiences both stream-wise and span-wise deformations. Similarly, the flap and flow frequencies are perceived from the coupled analysis and are compared with the experimental data. Moreover, the drag coefficient is computed for a given range of Reynolds number indicating reduction in drag induced by flap bending. A minimum value of 1.22 is achieved at highest Re, indicating a 29% decrease in comparison to the rigid flap. Therefore, the findings of present research could be helpful in designing thin flexible structures for flow control processes and artificial systems.*

1 INTRODUCTION

The mutual interactions of flowing fluid and structure is a well-known characteristic of wide-ranging engineering and natural science applications. Dynamic behavior of lighter and flexible objects entails a rapid development in experiments and simulation models explaining the fluid-flexible body interactions. Similarly, afterbody flexible shapes as flow control strategies predict better aero/hydrodynamic performance [1]–[3]. As FSI methodology, the use of computational fluid dynamics (CFD) software based investigations is a part of literature since the very beginning of computational engineering and hence, lightweight objects such as cantilevers are examined at moderate Reynolds number [4]. Strong coupling and large eddy simulation (LES) are employed using OpenFOAM and deal. II. Time history of the tip displacements is presented, and wake dynamics of the immersed cantilever is analyzed to show

the large structural displacements. Coupling procedures applied for 3D transient problems address the interesting solid-fluid interaction and therefore represent both the conduct of structure and flow. Reviewing a numerical study with respect to the fatigue life of flexible structures, Richter's test case [5] of an elastic obstacle for turbulent flow conditions is investigated by Rege [6]. LES model is implemented to get a vibration history of the flexible wall, therefore estimating the fatigue failure. Also, various established benchmark cases are discussed by Mehl et al. [7] using two newfangled iterative coupling schemes for the same test case [5]. Also, flow around a flexible plate is simulated for low density ratio (ρ^s/ρ^f) of 0.678 for $Re = 1600$ by Kim et al. [8]. As a result, the mean drag coefficients and the displacements of the free end of the plate are compared with the previous experimental and numerical investigations. Research outcomes specify that the present findings agree well with the literature [9], [10] showing the effectiveness and accuracy of the presented scheme.

To highlight the importance of flexible structures as passive wake control devices, flap-flexible plate system is examined for a D-shaped blunt body wake manipulation [11], [12]. Two-dimensional (2D) FSI simulations are offered by OpenFOAM for $Re = 12{,}000$. Plate deflection, drag force and near-wake flow are estimated for aligned flow conditions and are compared with experimental results. Similarly, coupled dynamics of a thin elastic structure and flow is carried out using ANSYS Workbench to predict the bending behavior of a flexible flap [13]. Resulting bending lines and the maximum tip deflections for different flap alignments and thickness are validated for transient situations. Reliable numerical results for 3D flapping applications are introduced for two-way coupled FSI problems encountering low Reynolds number. In comparison with the current work, laminar flow is investigated previously in [13] and consequently in the existing paper the dynamics of flexible flap is considered in further detail for crossflow conditions.

The literature survey shows the purpose of flexible objects for an extensive range of practical applications. Despite the recent significant research, the transient dynamics of flapping structures need still more to be discovered i.e., the response of a thin flexible structure for turbulent flowing applications in the subject range of Re. Also, current numerical approach is offered to explain and visualize the complexity of 3D flow problems across moving objects for crossflow problems. The particular objectives are to: (1) extend the 3D numerical investigations developed in [13] for turbulent flow conditions, (2) predict the flapping for hydrodynamic applications and corresponding flap and flow frequencies, (3) estimate the drag coefficient for flexible structures in comparison to the rigid ones, and (4) validate against measured PIV data. The research work is split into the following subsection. Section 2 explains the research procedures, computational domain, and corresponding numerical method. Section 3 offers the validation of the flexible flap, numerical outcomes and discussions followed by the conclusions in Section 4.

2 MATERIAL AND METHOD

For the investigation of FSI across elastic structures, a series of PIV measurements is carried out in an open water channel for a single flap case. Simulations are performed further to model the fluid-solid dynamics and validate the mutual response of fluid and structure. The experimental setup and numerical settings are explained in the following subsections.

2.1 Experiments

The experimental setup is designed to assess the flap profile made up of silicon rubber (Elastosil RT 601, Wacker Chemie, Germany) in an open water channel. The total channel is 5000 mm in length, 405 mm in height and 309 mm in width. The flap is mounted vertically downward normal to the flow direction and is clamped to a plate with one end free. Flap profile and bent description are shown in Figure 1. Experiments are performed by varying the flow rate of the channel, i.e., $Q \in [10{,}100]\ m^3/hr$, yields the corresponding flow velocity of $u \in [0.0359{,}0.359]\ m/sec$. The Reynolds number based on the width of the flap, w ,is defined as $\mathrm{Re} = \rho_f u \mathrm{w}/\mu \in [700{,}7000]$, where ρ_f is the fluid density and is μ the dynamic viscosity. Similarly, Reynolds number based on the channel width, Re_D, ranges from 11,000 - 110,000. The flow field in the surroundings of the flap is described by establishing 2D planer PIV measurements in different orientations: vertical plane and horizontal planes. The respective planes describe the two diverse views of the flap i.e., side and bottom respectively. Velocity distribution around the flap is assessed and resulting averaged as well as time-resolved (TR) velocity vectors are evaluated to present the flow unsteadiness in the flap vicinity. Further detail of measurements can be found in [14]. Moreover, the experimental images are turned by 180^o for consistency with the simulations.

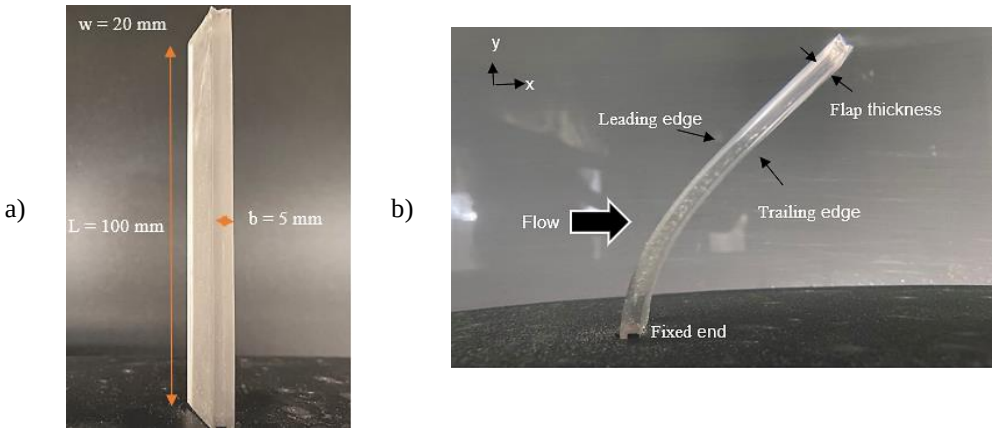

Figure 1: a) Flap configuration in a water channel (aspect ratio $L/w = 5$), b) Flap deformation in stream-wise direction, $Re = 7000$

2.2 Computational Model

To pursue the FSI simulations based on experimental conditions, both finite element (FE) analysis and computational fluid dynamics (CFD) models are independently designed in ANSYS Workbench. Model, mesh, boundary conditions and solvers are defined individually for solid and fluid. The geometry of the whole field is modeled in the ANSYS Design Modeler that defines a rectangular flow domain. The corresponding immersed flap is supposed to be mounted on the plate and engrossed in the fluid (Figure 2a). Afterwards two-way FSI coupling is introduced by means of ANSYS System Coupling. The structural domain, fluid domain and system coupling are discussed individually in the upcoming sections.

2.2.1 Structural domain:

To model the identical conditions as those in experiments, boundary conditions, model properties and dimensions are defined properly. The flap is designed in 'Transient Structural' (ANSYS Mechanical) by FE analysis. The boundary conditions for flap are defined with 'Fixed support' indicating the fixed end of the flap, while the other free walls are designed as 'Fluid Solid Interface' defining the leading and trailing edges of the flap as shown in Figure 2b. Linear elastic model is chosen for the flap and for the FE mesh generation, grid dependence is achieved by varying the hexahedral cells from 80 - 900 along the flap profile. Finally, the flap with 250 cells is chosen to run the simulations to save the computational time. The materials parameters are precisely defined in consistent with experimental conditions and are listed in Table 1.

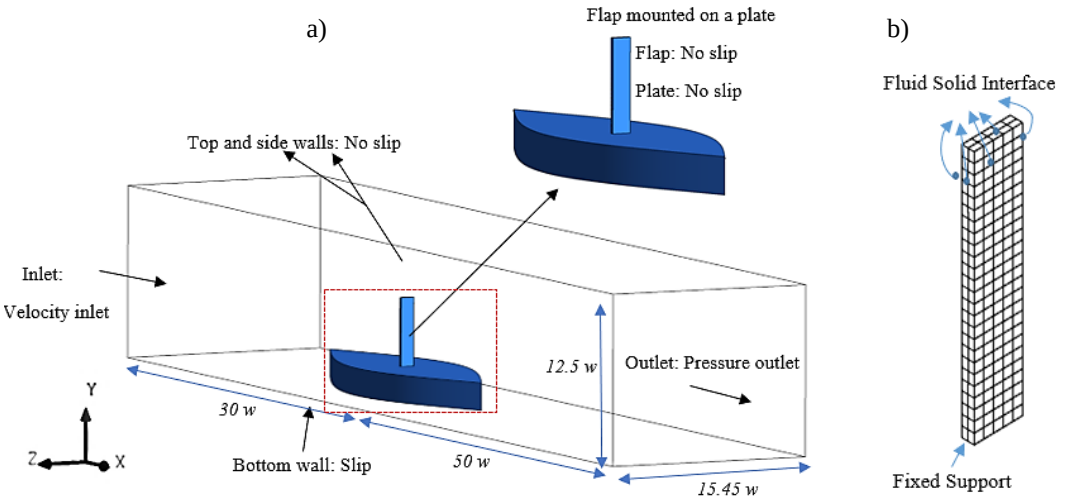

Figure 2: Numerical model in ANSYS Workbench a) A schematic of rectangular fluid domain and boundary conditions of flow around an elastic flap, b) Structural mesh and boundary conditions in FE analysis

2.2.2 Fluid domain:

To reproduce the experimental measurements in numerical simulations, the fluid domain is evaluated by CFD modeling with 'Fluent' solver. The domain is meshed by a tetrahedron unstructured mesh with higher mesh resolution around the flap. The mesh independence is checked by varying with the cells from 750,000 to 1.4 million and the mesh with highest cell count is selected for performing the final simulations. The boundary conditions for the fluid domain are taken as: 'no slip' walls for plate, flap, top and lateral sides of the channel. 'slip' boundary wall is assigned to the bottom and the 'velocity inlet' is given for the inlet conditions, whereas at the downstream 'pressure outlet' is chosen with the relative pressure of 0 Pa (see Figure 2a). To model the 3D unsteady incoming turbulent flow, the shear-stress transport (SST) k-ω turbulence model is used with a pressure-based coupled solver. To define the dynamic meshing, both smoothing and remeshing settings are implemented. The interface is taken as 'system coupling' in the dynamic mesh zone with a cell thickness of $2mm$ along the

wall. Also, the second-order upwind scheme is used to discretize the transport equations and second-order implicit transient formulation is implemented. The mesh resolution is shown in Figure 3.

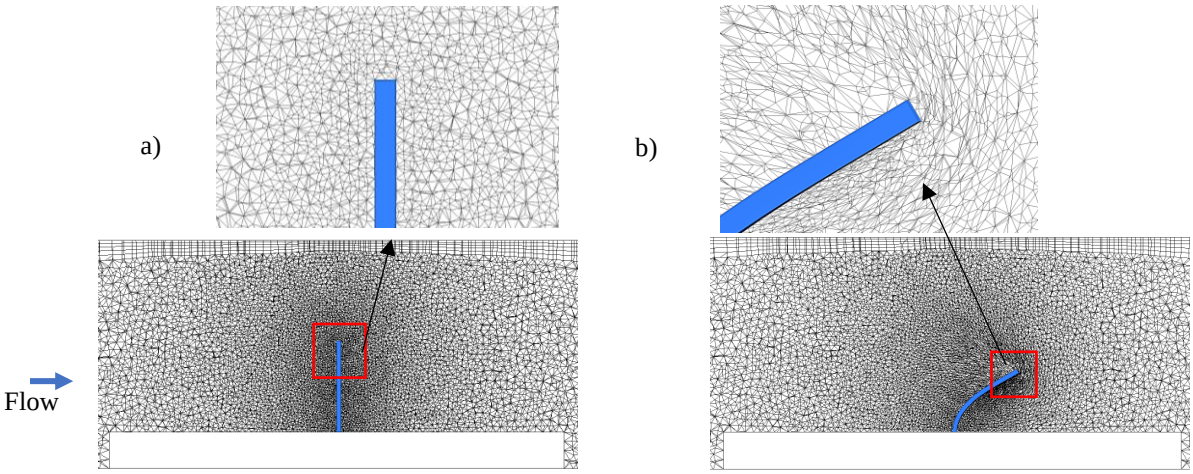

Figure 3: a) Undeformed mesh at initial time step, b) Deformed mesh at time $t = 5sec$, $Re = 7000$

Table 1: Computational parameters

Material	Property	Value	Units
Fluid-Water	Free stream velocity (u)	0.0359 – 0.359	m/sec
	Level (H)	250	mm
	Width (D)	309	mm
	Reynolds number (Re_D)	11,000- 110,000	
	Reynolds number (Re)	700 -7000	--
	Dynamic viscosity (μ)	1.002×10^{-3}	Kg/msec
Structure-Flap	Length (L)	100	mm
	Width (w)	20	mm
	Thickness (b)	5	mm
	Young's modulus (E)	1.23	MPa
	Shear modulus	0.47	MPa
	Poisons ratio (ν)	0.3	
	Mass ratio (ρ_s/ρ_f)	1.02	--

2.2.3 System coupling

The mutual interaction for FSI simulations is completed by defining a 'System coupling' between 'Fluent' and 'Transient Structural' solvers. For this purpose, data transfers are specified to transmit the information i.e. fluid pressure computed by the 'Fluent' and the structural deformation computed by the 'Transient Structural' thus forming two-way coupled FSI. Moreover, to achieve a stable flap movement and fluid remeshing, a time step size, Δt, of

0.001 sec is selected for the coupled simulations. The present simulations are conducted at the maximum CFL number of 0.10 and 1.73 respectively for lowest and highest flow velocities.

3 RESULTS AND DISCUSSIONS

3.1 Flap movement

The flap motion is observed for Re = 700 – 7000 for interpretation of flow-structure interactions. For lower Re i.e., $Re = 4000$, flap deforms initially and reaches a steady state. However, at higher Re it further starts oscillating in span-wise direction and resulting oscillations increases as Re increases. Hence, the flap exhibits multi-axis bending both in stream-wise direction in (xy) plane and similarly span-wise direction in (xz) plane. The two different flap motions are shown in Figure 4.

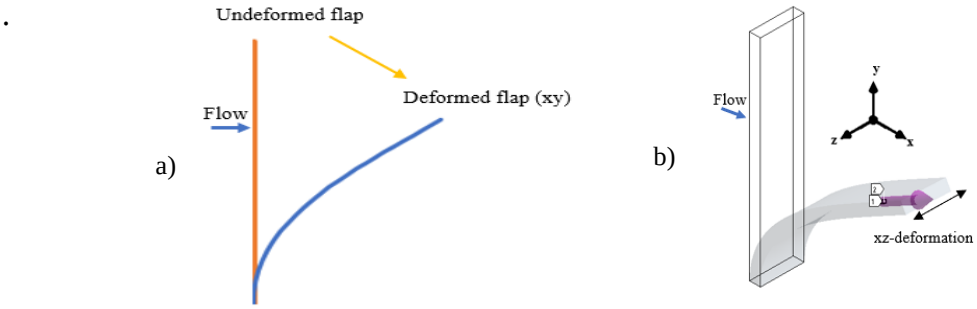

Figure 4: a) Undeformed flap, b) Deformed flap, $Re = 7000$

Total structural deformation is processed by ANSYS Transient Structural and depicts the resulting deformation in all three directions, namely, x, y and z respectively. The resulting time-dependent total deformation of flap is shown in Figure 5(a). The flap deformation is influenced by Re, as shown for lower Re it reaches a maximum value and then becomes steady. However, for higher Re, it progressively increasing and also shows oscillating behavior in span-wise direction. Similarly, the comparison of normalized maximum structural deformation in stream-wise direction (normalized with the flap length) is shown in Figure 5(b). Subsequent deformation (x_{max}) occurs at flap free-end i.e., flap tip and features an increase with Re. The resulting trend shows barely any prominent deflection for the lowest Re, whereas it reaches a peak value of 72 mm for $Re = 7000$ in the investigated range of $700 < Re < 7000$.

To interpret the measurements further and determine the bending shape of the flap, xy-bending line for higher Re is depicted in Figure 5(c). The results show that for maximum flow velocity ($Re = 7000$), the flap deflection is nearly $1/3$ of its length that is $y_m/L = 0.7$ for FSI simulations. Also, the x-deformation (x_m/L) at highest Re is reaching twice to that of $Re = 4300$. Covering the higher range of Re, the results from experiments and simulations predict the similar bending behavior of the flap and are in a good agreement. Moreover, to investigate the bending curves of the flap, the motion is examined only at the leading edge. Likewise, the time-series for flap movement (z/L) indicates the extreme flap positions in span-

wise direction. Both measurements and simulations show an oscillating behavior however, for measurements flap settles differently in time and therefore no fixed extremity is defined.

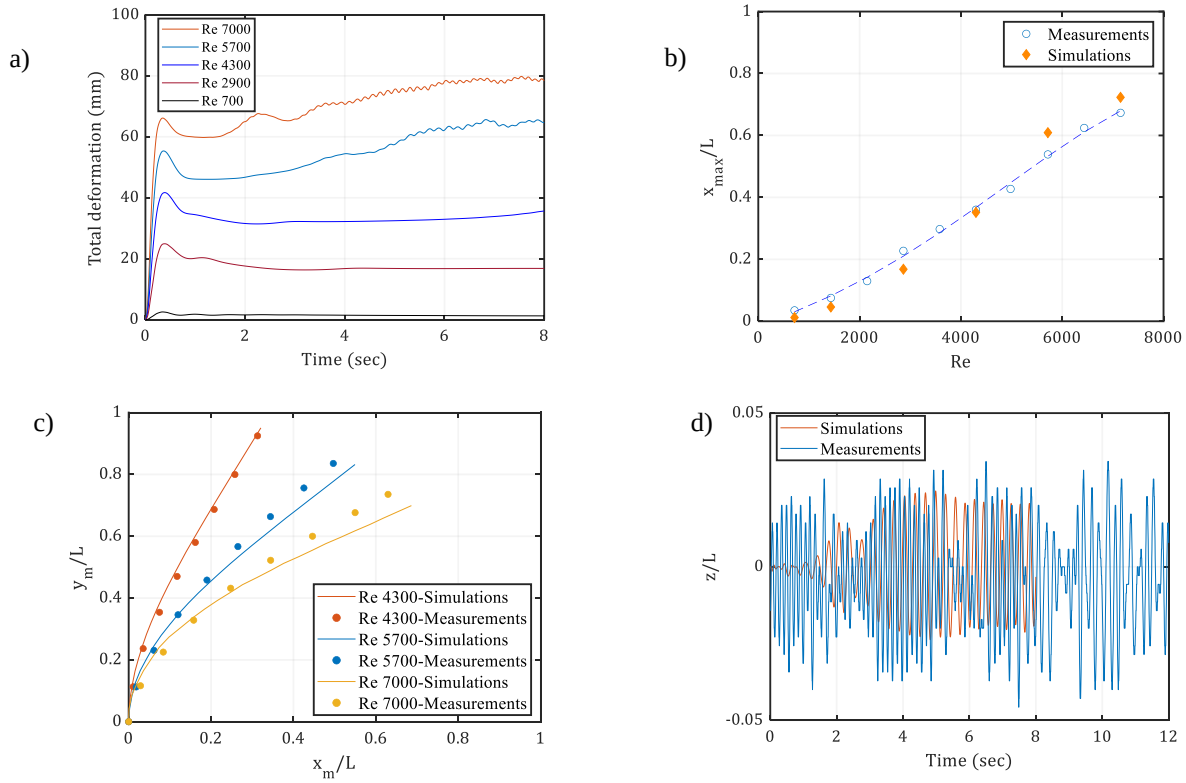

Figure 5: a) Time-series of total deformation over Re, PIV measurements vs simulations: b) Maximum flap tip deflection (x_{max}) over specified range of Re, c) Mean xy-bending line (x_m, y_m) for higher Re, d) Flap displacement in span-wise direction over time for $Re = 7000$

To investigate the unsteady structural response and its influence on flow oscillations, flap frequency is analyzed initially both for PIV measurements and simulations. The Fast-Fourier transform (FFT) on displacement time-series (Figure 5d) is performed to achieve the resulting frequency spectrum as shown in Figure 6. A single frequency peak at 3.39 Hz is depicted from

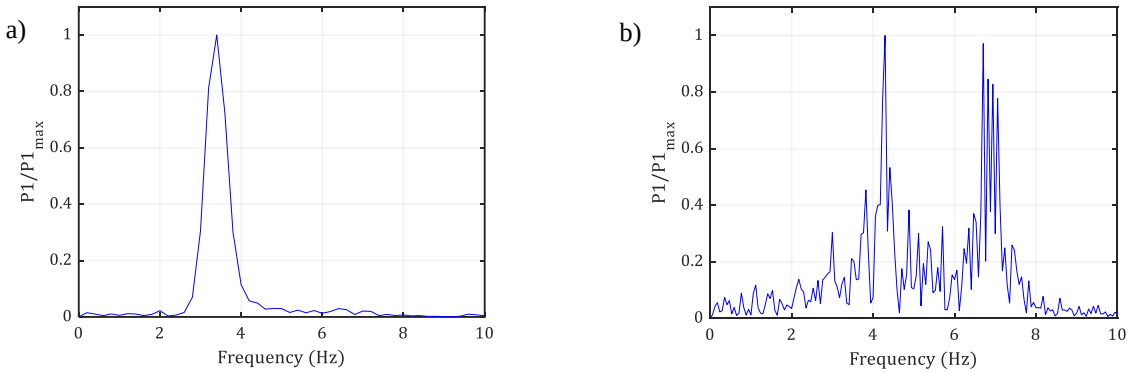

Figure 6: Spectrum of flap frequency in span-wise direction, a) simulations, indicating highest peak at 3.39 Hz, b) PIV measurements show two dominant peaks at 4.29 Hz and 6.70 Hz, $Re = 7000$

the numerical data, while frequency spectrum of measurements indicates two dominating peaks at 4.29 Hz and 6.70 Hz respectively. Though both the measurements and simulations indicate the oscillating behavior, the difference may arise since long term flap behavior in simulation is still to be investigated for further computational time. Besides, the flap flexibility and frequency are further helpful in investigating the flap-flow behavior (Section 3.2).

3.2 Flow visualization

It is well understood that the flow past a bluff body leads to a phenomenon of vortex shedding at higher Re. Also, 2D cylindrical bodies and 3D spherical structures indicate the wake transitions at $Re \geq 100$ and associated FSI. Likewise, square cylinders also show definite wake characteristics and Re dependence [15], [16]. Therefore, to understand the 3D wake region behind a flexible rectangular cylinder alike structure, simulations are performed across a thin elastic flap for a specified range of Re. Corresponding results show that flap deformation significantly affects the flow dynamics and eventually flow separation. So as to explain the mutual interaction of flap and flow, instantaneous snapshots of vorticity in a mid-cut section of the flap bent for a horizontal (xz) plane are depicted in Figure 7a. The detachment occurs just behind the flap leading edge and the flow finally separates at the trailing edge of the flap. The sequence of vortex formation is shown for lowest, medium and highest Re. Hence, when the flap and fluid are coupled together, they appear to establish a collective response which ultimately influences the flow formations and the wake patterns. Therefore, the vortex visualization in terms of the Q-criterion for a deforming flap is shown in Figure 7b. Initially, the flow is separating from the mounting plate and then afterwards separation occurs across the free end of the flap. The periodic vortical structure originates from the flap tip and hence swirling downstream. Also, the stronger deformation of the flap at higher Re alters the wake significantly and alternating flow pattern in the flap wake is formed.

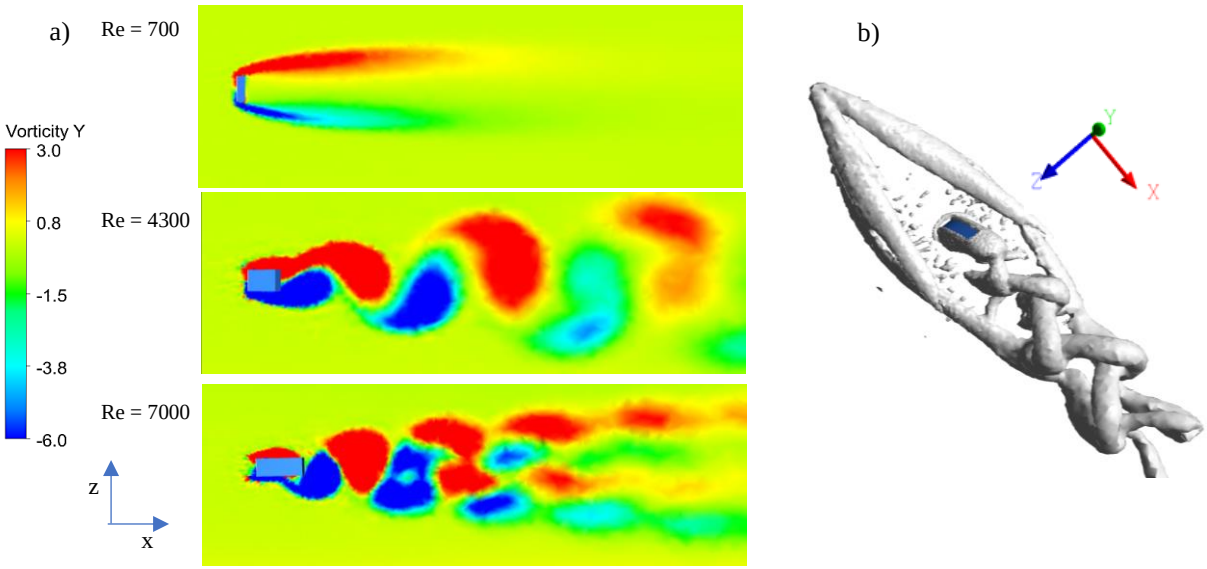

Figure 7: a) Span-wise vorticity contour plot in plane y = mid-cut section of flap bent for $Re = 700$, $Re = 4300$ and $Re = 7000$, b) Wake structure at $Re = 4300$

3.3 Evaluation of flow data

3.3.1 Vortex shedding frequency (f_s)

The periodic nature of flow is estimated by vortex shedding frequency, through FFT of flow velocity (u_x) at different probe locations in the flap downstream for $Re = 7000$. Corresponding probe locations and a sample of velocity fluctuation are shown in Figure 8(a, b). The subsequent comparison of frequency spectrum at location 1 is represented in Figure 8(c, d) respectively. As shown for FSI simulations, the dominating peak occurs at 3.59 Hz and two smaller peaks at 0.1998 Hz and 6.59 Hz respectively. Similarly, for the measurements the dominating peak occurs at 3.9 Hz along with another higher peak at 0.49 Hz. Consequently, for location 2, two dominating peaks at 0.19 Hz and 3.9 Hz are observed for the measurements, while for simulations it is the same as location 1. The peaks at 0.19 Hz in experiments and simulations relate the stream-wise movement of the flap. However, the generation of small-scale vortices are surely present in the experimental signal indicating the multiple sharp peaks i.e., at 0.49 Hz and 0.33 Hz. Also, the resulting frequency signals emphasize the influence of flap motion for the coupled FSI problem specifies the flap-flow frequency concerning the span-wise movement of the flap (Section 3.1).

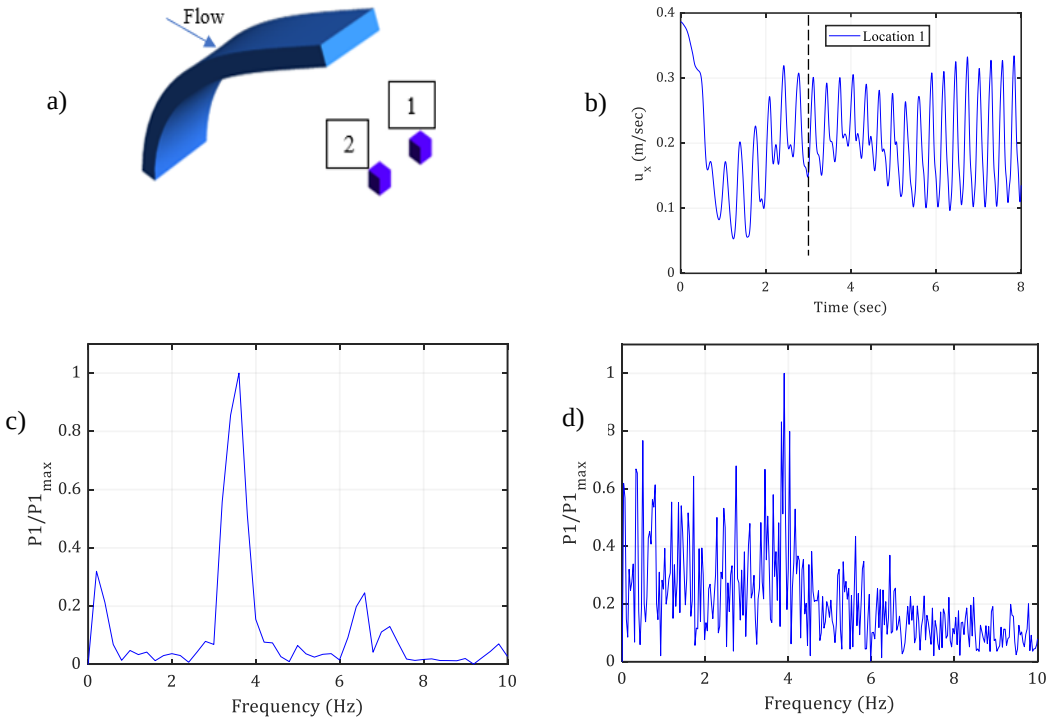

Figure 8: a) Location of probes 1,2 for a horizontal plane at mid-cut section of the flap bent, b) Velocity (u_x) variation over time at location 1, dotted line shows the time span for FFT c) Frequency spectrum of simulations at location 1 showing a highest peak at 3.59 Hz, d) Frequency spectrum of measurements showing a highest peak at 3.9 Hz for location 1

Furthermore, the Strouhal number is defined based on the flap width and incoming flow velocity as $St = f_s w/u$ [4] and is calculated based on the frequency spectrum attained at each

location as described in Section 3.3.1 for the maximum Re . The St reaches a maximum value of 0.19 by FSI simulations, indicating the dominant flap motion and maximum shedding frequency. The resulting values are compared with the experimental data as well and the current numerical and experimental values are in good agreement i.e. experimental value of $St = 0.2$ is attained at highest Re. Although data for rigid square cylinder indicates a constant value of St= 0.13 for the current *Re* range [16], [17].

3.3.2 Drag coefficient

The time-mean drag coefficient is defined as $\bar{C}_d = 2\,\bar{F}_d/u^2 A\rho_f$ [16], where $\bar{F}_d$is the time-mean instantaneous drag force, A is the undeformed area of the flap and ρ_f is the fluid density. The instantaneous drag F_d is recorded at every time step from initial time until the end of a simulation. In Figure 9a, $\bar{C}_d$ is plotted as a function of Re for current investigation of a flexible flap. An increased flexible response corresponding to a lower value of $\bar{C}_d$ reaches a minimum of 1.22 at $Re = 7000$. It is observed that with an increase in Re, fluid pressure forces are more significant and viscous drag shows least contribution with regard to the drag force for current crossflow conditions. It is also of interest to compare flexible flap with rigid square cylinder, in terms of dependence of $\bar{C}_d$ on Re and therefore is included in Figure 9a as well. The corresponding literature data by Bai [16] remains constant at $\bar{C}_d$ = 2.21 for $Re > 2000$. Though this trend of stationary square body differs from the existing flap as expected flexibility and bending shape present a smaller profile to the incoming flow and induce a drag reduction. Also, as described in Section 3.1 that the flap exhibits multi-axis bending and oscillates in response to the incoming fluid, therefore, the current observations of the flexible and rigid flap cases at $Re = 7000$, reports a decrease in $\bar{C}_d$ to 29%. Figure 9b represents the time evolution of drag coefficient for final period $I = [0, 1]$ aimed at minimum and maximum Re. For highest Re, fluctuating drag coefficient indicates the dominant flap oscillations and alternating wake structure separating from the flap edges as compared to the lowest Re.

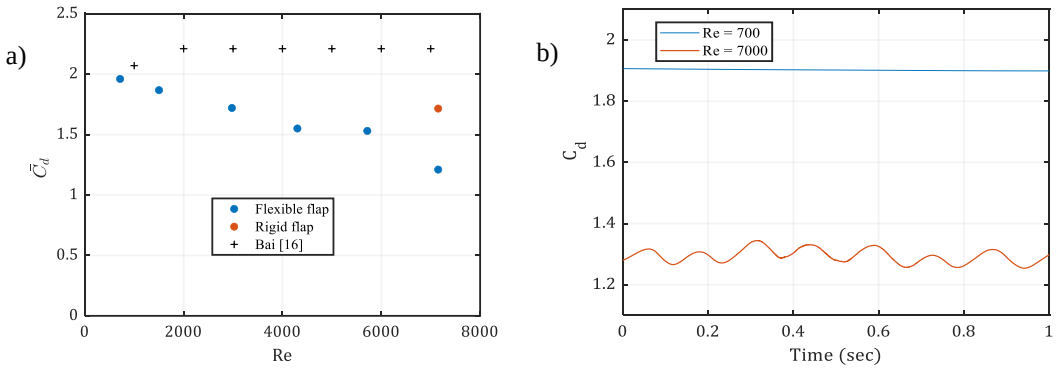

Figure 9: a) Dependence of $\bar{C}_d$ on Re, b) Time-series of C_d for $Re = 700$ and $Re = 7000$

4 CONCLUSIONS

In this work, a numerical method is presented to analyze FSI in turbulent flow for crossflow applications. The motion of a thin flexible flap in an open water channel is simulated and compared with PIV measurements. The numerical procedure is meant for the experimental conditions for medium to high Re, $700 < Re < 7000$. Flap bending line and corresponding flap and flow frequencies are predicted and are compared with the measurements. It is found that the flap exhibits motion in both stream-wise and span-wise directions. For the minimum Re, the flap is observed to be nearly undeformed and does not show any notable deflection whereas for the maximum Re, it is deflected by $1/3$ of its undeformed length. Similarly, xy-flap bent shows an increase with increase in Re and the bending behaviors attained by current simulations are very close to the measurements. Also, study includes the 3D flow disturbances effected by the flap flexibility and shedding frequency at highest Re. Particular flap frequency is close to that of flow frequency indicating the coupled fluid-structure motion. The highest St of 0.19 is achieved from the present simulations and is comparable with the measurement value of 0.21. For current 3D simulations, the flap bending profiles and Strouhal number are in good agreement with existing experiments. Flexibility effects are surely the reason for the difference between the literature data for rigid square structure verses present findings. Finally, the variation of drag coefficient over *Re* is also presented for the present numerical study. To conclude, the offered FSI data set aim to design 3D interactions and explain the flow physics around thin elastic structures in order to narrow the literature gap for the subject range of Re.

5 ACKNOWLEDGEMENT

The current research work is supported by the funding from the funds of the Freistaat Sachsen Germany, grant number Landesstipendium. The authors gratefully acknowledge Mrs. Katrin Bauer, Mr. Johannes Burkert for carrying out the PIV measurements and Mr. Marcel Selent for performing the cantilever bending test for the flap.

REFERENCES

[1] K. R. Sharma and S. Dutta, “A review on unsteady fluid-flexible structure interaction,” *J. Flow Vis. Image Process.*, vol. 29, no. 2, 2022.

[2] H. Zhang, Y. Zhao, X. Tian, X. Wang, and H. Liu, “Symmetry breaking of a closed flexible filament behind a rigid plate at low Reynolds numbers,” *Phys. Fluids*, vol. 35, no. 2, 2023.

[3] C. Wang, H. Tang, and X. Zhang, “Fluid-structure interaction of bio-inspired flexible slender structures: A review of selected topics,” *Bioinspir. Biomim.*, vol. 17, no. 4, p. 41002, 2022.

[4] J. Lorentzon and J. Revstedt, “A numerical study of partitioned fluid-structure interaction applied to a cantilever in incompressible turbulent flow,” *Int. J. Numer. Methods Eng.*, vol. 121, no. 5, pp. 806–827, 2020.

[5] T. Richter, “Goal-oriented error estimation for fluid–structure interaction problems,”

Comput. Methods Appl. Mech. Eng., vol. 223, pp. 28–42, 2012.

[6] K. Rege and B. H. Hjertager, "Application of foam-extend on turbulent fluid-structure interaction," in *IOP Conference Series: Materials Science and Engineering*, 2017, vol. 276, no. 1, p. 12031.

[7] M. Mehl, B. Uekermann, H. Bijl, D. Blom, B. Gatzhammer, and A. Van Zuijlen, "Parallel coupling numerics for partitioned fluid–structure interaction simulations," *Comput. Math. with Appl.*, vol. 71, no. 4, pp. 869–891, 2016.

[8] W. Kim, I. Lee, and H. Choi, "A weak-coupling immersed boundary method for fluid–structure interaction with low density ratio of solid to fluid," *J. Comput. Phys.*, vol. 359, pp. 296–311, 2018.

[9] F.-B. Tian, H. Dai, H. Luo, J. F. Doyle, and B. Rousseau, "Fluid–structure interaction involving large deformations: 3D simulations and applications to biological systems," *J. Comput. Phys.*, vol. 258, pp. 451–469, 2014, doi: https://doi.org/10.1016/j.jcp.2013.10.047.

[10] M. Luhar and H. M. Nepf, "Flow-induced reconfiguration of buoyant and flexible aquatic vegetation," *Limnol. Oceanogr.*, vol. 56, no. 6, pp. 2003–2017, 2011.

[11] C. García-Baena, J. I. Jiménez-González, and C. Martínez-Bazán, "Drag reduction of a blunt body through reconfiguration of rear flexible plates," *Phys. Fluids*, vol. 33, no. 4, 2021.

[12] C. García-Baena, J. M. Camacho-Sánchez, M. Lorite-Díez, C. Gutiérrez-Montes, and J. I. Jiménez-González, "Drag reduction on a blunt body by self-adaption of rear flexibly hinged flaps," *J. Fluids Struct.*, vol. 118, p. 103854, 2023.

[13] T. Bano, F. Hegner, M. Heinrich, and R. Schwarze, "Investigation of Fluid-Structure Interaction Induced Bending for Elastic Flaps in a Cross Flow," *Appl. Sci.*, vol. 10, no. 18, 2020, doi: 10.3390/app10186177.

[14] T. Bano, J. Burkert, and R. Schwarze, "'An experimental study to investigate the response of a flexible flap interacting with a fluid flow,'" in *Fachtagung "Experimentelle Strömungsmechanik" 6.–8. September 2022, Ilmenau*, 2022, p. 8, [Online]. Available: https://gala-ev.org/images/Beitraege/Beitraege2022/beitraege.html.

[15] M. C. Thompson, T. Leweke, and K. Hourigan, "Bluff bodies and wake–wall interactions," *Annu. Rev. Fluid Mech.*, vol. 53, pp. 347–376, 2021.

[16] H. Bai and M. M. Alam, "Dependence of square cylinder wake on Reynolds number," *Phys. Fluids*, vol. 30, no. 1, 2018.

[17] A. Okajima, "Strouhal numbers of rectangular cylinders," *J. Fluid Mech.*, vol. 123, pp. 379–398, 1982.